Spatial Sensitivity Analysis for Urban Hotspots using Cell Phone Traces

Journal Title
XX(X):1–25

DOI: 10.1177/ToBeAssigned
www.sagepub.com/
SAGE

Abstract

Urban hotspots can be used to model the structure of urban environments and to study or predict various aspects of urban life. An increasing interest in the analysis of urban hotspots has been triggered by the emergence of pervasive technologies that produce massive amounts of spatio-temporal data including cell phone traces (or Call Detail Records). Although hotspot analyses using cell phone traces are extensive, there is no consensus among researchers about the process followed to compute them in terms of four important methodological choices: *city boundaries, spatial units, interpolation methods and hotspot variables*. Using a large scale CDR dataset from Mexico, we provide a systematic spatial sensitivity analysis of the impact that these methodological choices might have on the stability of the hotspot variables at both *inter-city* and *intra-city* levels.

Keywords

Spatial sensitivity analysis, Urban hotspots, Cell phone traces

Introduction

Urban environments can be characterized using different approaches, such as land use, mobility matrices, or activity centers (*a.k.a.* hotposts). The recent availability of pervasive technologies has triggered new ways of studying cities using different data sources such as social networks, GPS, public transport information and also cell phone traces.

Cell phone traces (or Call Detail Records, CDRs) are collected by telecommunication networks for billing purposes and provide - among other features - spatio-temporal data about mobility behavior. Although the locations are not in GPS format, but rather represent the location of cellular towers, CDR data has proved to be useful in modeling a variety of human mobility behaviors such as analyzing daily patterns to understand the *pulse* of a city (Ratti et al. 2006; Calabrese et al. 2011; Reades et al. 2007; Gao 2015; Ahas et al. 2015); investigating the correlation between human mobility patterns and land-use patterns as well as urban functions (Reades et al. 2007, 2009; Bachir et al. 2017; Noulas et al. 2013; Tu et al. 2017); clustering geographic units as dense regions to understand city dynamics at large scale (Vieira et al. 2010; Doyle et al. 2014); or detecting events within a city, *i.e.,* large gatherings of people within a short period of time (Traag et al. 2011; Dong et al. 2015).

A critical area in mobility behavior analysis is the identification of activity centers or dense regions *a.k.a.* hotspots, defined as regions with high concentration of individuals for a given period of time (Ratti et al. 2006; Vieira et al. 2010; Louail et al. 2014; Hoteit et al. 2014). Hotspot analyses using CDR data are generally carried out in two different scenarios (1) modeling, with a focus on analyzing the urban structure, such as the quantification of the urban sprawl or compactness of cities (Louail et al. 2014; Xu et al. 2019); or the analysis of the spatio-temporal evolution of popular locations for a given region (Zuo and Zhang 2012; Ghahramani et al. 2018); and (2) prediction, with a focus on the analysis of the predictive power of dense regions with respect to a given variable; for example, high footfall (number of estimated visits) in a region has been associated to high crime (Bogomolov et al. 2015; Traunmueller et al. 2014), or large numbers of individuals at night or work times have been associated to the identification of home (residential) and work locations (Isaacman et al. 2012; Becker et al. 2011). These studies are often carried out at two different spatial scales: *intra-city*, where researchers focus on models or predictions for a given city (Ratti et al. 2006; Reades et al. 2007); and *inter-city*, where researchers focus on comparing behaviors across cities (Louail et al. 2014; Ahas et al. 2015).

Although hotspot analyses using cell phone traces are extensive, there is no consensus among researchers about the process followed to compute them in terms of three important features: (i) *city boundaries* used to define the area under study *e.g.,* some researchers use metropolitan areas (Louail et al. 2014) that represent *cities* as labor market areas comprising commuting behaviors, while others use a smaller entity - the core municipality - which represents the physical boundary of a city rather than its economic activity, and which is generally contained within a metropolitan area together with other non-core municipalities (Ratti et al. 2006; Demographia 2020); (ii) *spatial units* considered to compute the hotspots, which in the literature range from using Voronoi polygons that simulate cell phone coverage areas (Vieira et al. 2010; Trasarti et al. 2015; Gao 2015); to uniformly distributed grids (Louail et al. 2014; Isaacman et al. 2012; Douglass et al. 2015; Candia et al. 2008; Balzotti et al. 2018; Sagl et al. 2014; Reades et al. 2009, 2007; Tu et al. 2017); or census tracts (Doyle et al. 2014; Bachir et al. 2017), with the latter two approaches requiring the use of *interpolation methods* (Bachir et al. 2017; Peredo et al. 2017; Ahas et al. 2015; Kubíček et al. 2019) to distribute individuals associated to a given cellular tower across grids or census tracts; and (iii) *hotspot variables* used to measure and characterize the computed hotspots, such as the total number of hotspots for a region or hotspot compactness measures (Fryer and Holden 2011; Angel et al. 2010). The combination of these different features could produce significant differences in the hotspots identified, which could in turn provide conflicting findings.

In this paper, we provide a spatial sensitivity analysis of the impact that the choice of a given set of city boundaries, spatial units and interpolation methods might have on the stability of the hotspot variables computed using cell phone traces (CDR). The recommendations of these analyses will provide guidelines for researchers looking to identify the most stable combination of parameters that will preserve the stability of the CDR-based hotspots independently of the city boundaries, spatial units and interpolation methods selected; and will also pinpoint into risky combinations of features that might produce non-stable, CDR-based hotspot measures. Additionally, these recommendations will also guide researchers into whether results across papers can be compared or not, based on the reported stability of certain combinations of features.

The systematic analysis will be carried out for two cases: inter-city and intra-city, where most of the related literature in CDR-based hotspot analyses has focused. Inter-city analyses will evaluate the stability of the city-rankings, based on a given hotspot variable, across different combinations of city boundaries,

spatial units and interpolation methods; while intra-city analyses will assess the stability of a hotspot variable - computed hourly and represented as a 24 hour vector - across different combinations of city boundaries, spatial units and interpolation methods. Next, we will review some related work, followed by our methodology in depth. Then we will present and discuss the results.

Related Work

As discussed in the Introduction, hotspot analyses are typically carried out at inter-city and intra-city scales, and with two complementary research objectives in mind: (1) to model the urban structure or human dynamics, or (2) to understand the predictive relationship of hotspots with other aspects of urban life. When modeling human dynamics at the *intra-city* level, researchers have focused on the structure for a given city overtime. Rubio et al. (2013) and Vieira et al. (2010) visualized the temporal evolution of hotspots to demonstrate the convergence and divergence pattern of a city. Reades et al. (2007) and Gariazzo et al. (2019) clustered the spatial units based on the temporal variation of density to identify regions with different temporal patterns. At the *inter-city level*, researchers generally compare the urban structure among different cities. Louail et al. (2014) used number of hotspots and compacity coefficient to quantify the hotspots for each city; Xu et al. (2019) computed proximity and agglomeration and Li et al. (2014) used normalized mass moment of inertia to measure the compactness of cities. On the other hand, when using hotspots as a tool to study or predict different aspects of urban life researchers have shown that, at the *intra-city* level, dense areas are associated with high volumes of crimes in London, UK (Bogomolov et al. 2015; Traunmueller et al. 2014). At the *inter-city* level, Louail et al. (2014) showed the number of hotspots is positively correlated with the cities' population. Xu et al. (2019) found a U-shape non-monotonic effect between the compactness of hotspots and GDP per km^2. Burton (2000) observed that compact cities tend to have higher crime rate; and Guo et al. (2019) showed a negative correlation between urban sprawl and income segregation. However, all these papers have divergent methodological choices for hotspot analyses, with often times unjustified choices for city boundaries, spatial units and variables used to quantify the hotspots. As a result, these approaches might suffer from the well known *modifiable areal unit problem* (MAUP) (Openshaw 1984), *i.e.,* the areal units (zonal objects) used in many geographical studies are arbitrary, modifiable, and studies like Strominger et al. (2016) suggest, these methodological choices could introduce conflicting findings if not carefully examined. Therefore, in our study, we will conduct systematical analysis of the impact from these methodological choices to provide insights about how to avoid potentially conflicting findings.

Methodology

Hotspot analyses using CDR data are critical to study city dynamics and the spatial structure of cities. To detect hotspots, researchers generally follow a set of common steps, although its implementation varies widely depend on research focus, application area or data availability. In this section, we will explain the different choices that researchers have in hand when computing hotspots, and we will describe the methodology we will use to assess the impact that the choice of varying feature combinations might have on the stability of a given hotspot measurement variable, both at the inter-city and intra-city levels.

Researchers generally follow these four steps to the identify the hotspots in a region: (i) define the city boundary of the city under study, (ii) define the type of spatial units used to compute hotspots, and estimate the population for each spatial unit, (iii) detect hotspots based on the estimated population, and

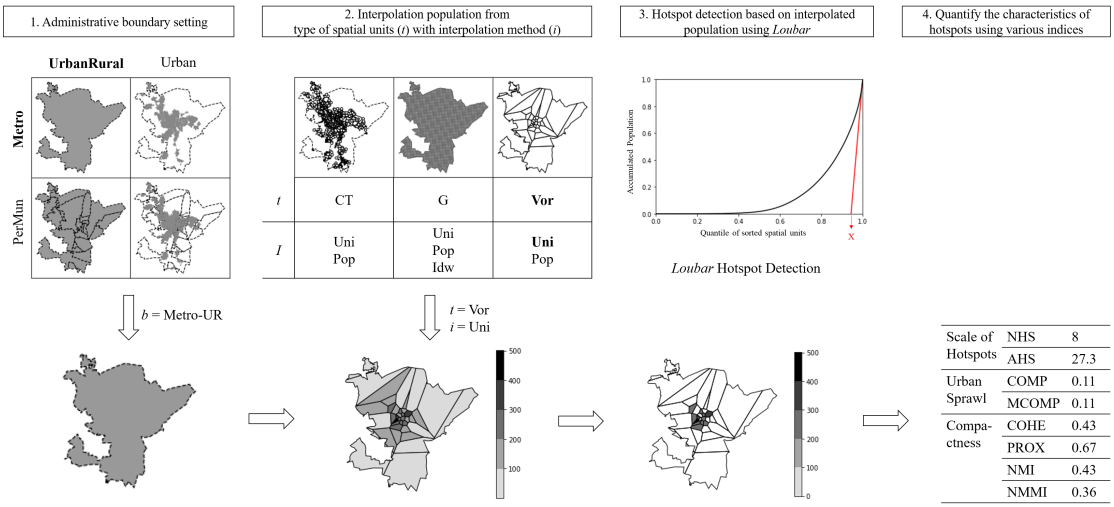

Figure 1. Hotspot Identification Process. The grey areas in Step 1 are the areas considered in each city boundary setting *e.g.,* the grey areas in Urban settings are urban areas, while the white areas are the rural areas. The outer boundary is the metro area boundary and the inner boundaries are the municipalities' boundaries.

(iv) compute hotspot indices to quantitatively characterize crowded regions in a city. Next, we explain each component in Figure 1 in detail.

City boundaries

The delimitation of cities or *urban* areas is in itself one of the traditional tasks in urban geography and planning (Ouředníček et al. 2018). Although not the focus of this paper, it highlights the importance of understanding the impact that different city delimitations might have on hotspot analyses. Most related studies focused on the computation of CDR-based hotspots consider two different dimensions.

The first one is the definition of the physical city boundary. While some researchers define cities by their metropolitan area (Louail et al. 2014; Gariazzo et al. 2019), others only consider the urban core (Ratti et al. 2006; Chen et al. 2018; Zhao et al. 2016; Schwarz 2010; Kubíček et al. 2019). Metropolitan areas are often defined as an aggregation of municipalities that share industry, infrastructure and housing, and that represent the *economic city* with a densely populated urban core area - that might span across multiple municipalities - and its surrounding rural, less-populated areas. On the other hand, municipalities are generally smaller spatial units embedded within a metropolitan area, with its urban core representing the physical boundary of the city and the region that has emerged historically as the most prominent in the metropolitan area (Demographia 2020). Therefore, when the term *city* is used in current CDR-based hotspot analyses, it is important to understand whether it refers only to the densely populated areas within a metropolitan area (Ratti et al. 2006; Chen et al. 2018; Zhao et al. 2016; Schwarz 2010); or to the metropolitan area as a whole, including both the densely populated urban area and its

less-populated, rural surrounding territories (Gariazzo et al. 2019; Le Néchet 2012; Louail et al. 2014). See *Urban* and *UrbanRural* columns in Figure 1.

The second dimension focuses on whether to treat the metropolitan area as a whole unit to compute hotspots, or to consider each embedded municipality independent of each other, albeit connected by secondary population flows. Since metropolitan areas delimit the economic city, with mobility flows between its core urban area and other regions, it makes sense to identify hotspots at that scale, which would mostly characterize the commuting population (Le Néchet 2012; Louail et al. 2014). However, by computing hotspots at that scale, local characteristics or economic structures of individual municipalities might be ignored. For example, non-core municipalities within a metropolitan area might be sub-centers for jobs in the region (Ouředníček et al. 2018). As a result, the mobility patterns characterizing these municipalities might be more affected by its internal flows that by movements to and from other municipalities (Gariazzo et al. 2019).

To carry out a comprehensive assessment of the different city boundary settings that are used by researchers when computing CDR-based hotspots, we propose to explore the following four settings: (i) *Metropolitan Area Urban-Rural* (Metro-UR), where hotspots are computed across the the whole metropolitan area that includes all urban and rural areas; (ii) *Metropolitan Area Urban* (Metro-U), where hotspots are computed across the whole metropolitan area which is defined exclusively by its urban areas; (iii) *Municipalities Urban-Rural* (PerMuni-UR), where hotspots are computed per individual municipality, and considering both urban and rural areas within the municipality; and (iv) *Municipalities Urban* (PerMuni-U), where hotspots are computed individually only for the urban areas within each municipality. The boundary setting is denoted as b with $b \in \{\text{Metro-UR, Metro-U, PerMuni-UR, PerMuni-U}\}$. An example of the four different boundary types are shown in Step 1 in Figure 1.

Spatial units and interpolation methods

Voronoi tessellation is a common spatial unit of choice when using CDR data to understand population dynamics (Vieira et al. 2010; Sevtsuk and Ratti 2010; Doyle et al. 2014; Trasarti et al. 2015; Gao 2015). For each cell tower c in the cell phone infrastructure, Voronoi tesselation is used to represent its spatial coverage or service area (see Figure 2). The assumption on which Voronoi tessellation is based is that users would always use the closest cell tower. In this way, researchers associate to a given Voronoi polygon v_c all the individuals that have been observed at that cell tower c. However, Voronoi polygons (Vor) are not the only type of relevant spatial unit. Some researchers have focused on spatial regularity and have chosen grids (G) (Louail et al. 2014; Isaacman et al. 2012; Douglass et al. 2015; Candia et al. 2008; Balzotti et al. 2018; Sagl et al. 2014) as the spatial units of interest, while others prefer to census tracts or blocks (CT) (Doyle et al. 2014; Bachir et al. 2017) because these are the same geographic units as census data and can represent the boundaries of neighborhoods to some extent. In this paper, we will denote the type of spatial unit as t with $t \in \{\text{CT, G, Vor}\}$.

Voronoi tessellation assigns a set of individuals to a given Voronoi polygon, and the number of individuals *i.e., the footfall*, is then used to compute hotspots. However, when using grids or census tracts, or when a Voronoi polygon needs to be clipped because it spreads outside the boundary of a city or a municipality, additional processing is required to assign the presence of individuals to a different spatial unit. Grid and census tracts polygons will overlap with Voronoi polygons, and as a result, interpolation methods that approximate the footfall in a given overlapping polygon area is required (see Figure 2 for an example). Similarly, clipped Voronoi polygons will require to approximate the footfall for any given

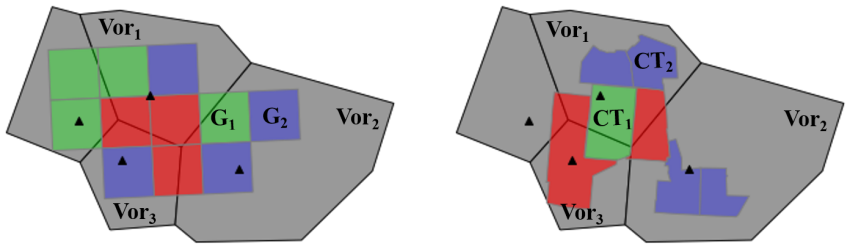

(a) Grids (b) Census tracts

Figure 2. An example of grids intersecting with Voronoi polygons (the underlying grey polygons). The locations of cell towers are represented as black triangles. Grids or census tracts in red, green and blue intersect with three, two and one Voronoi polygons, respectively. For example, G_1 intersects with Vor_1 and Vor_2, G_2 intersects with Vor_2, CT_1 intersects with Vor_1 and Vor_3 and CT_2 intersects with Vor_1.

sub-polygon. With that objective in mind, we explore three types of interpolation methods commonly present in the literature: uniform (Uni), population-based (Pop) and inverse-distance (Idw) (Louail et al. 2014; Bachir et al. 2017; Peredo et al. 2017). In this paper we will denote the interpolation methods as i with $i \in \{\text{Uni, Pop, Idw}\}$.

The most common interpolation method in the CDR literature is the uniform method (Uni) (Louail et al. 2014; Kubíček et al. 2019; Kang et al. 2012). This method assumes that all individuals are located within a given polygon uniformly. Therefore, the number of individuals in any grid or census tract polygon overlapping with a Voronoi polygon will be proportional to its area. Let $\boldsymbol{v}$ be the set of Voronoi polygons intersected with spatial unit u, v_c be the Voronoi polygon and n_c be the footfall in cell tower c, the interpolated footfall $n_{u,i=\text{Uni}}$ using the Uniform method for u is computed as follows:

$$n_{u,i=\text{Uni}} = \sum_{v_c \in \boldsymbol{v}} \frac{\text{Area}\left(\text{Intersection}\left(u, v_c\right)\right)}{\text{Area}\left(v_c\right)} \cdot n_c \tag{1}$$

The limitation of the Uniform method is that people are unlikely to be distributed over a spatial unit uniformly, especially for vast rural areas where people are less likely to be present. Therefore, researchers have used population-based methods (Pop) that distribute the footfall of a Voronoi polygon over a spatial unit proportionally to the population density *e.g.,* urban areas in the spatial unit are assigned larger numbers of individuals than rural areas (Bachir et al. 2017). The population-based method requires information about census population. Let the given census population distribution be at the census tract level, y_x be the shape and p_x be the population of the x-th census tract. The census population is assumed to be normally distributed within y_x, as no finer-grained information about population is available. Let S be an arbitrary polygon *e.g.,* a spatial unit or the intersection between a spatial unit and a Voronoi polygon. If S itself is a census tract, the population of S is straightforward. That is one of the reasons why some researchers prefer to use census tract as spatial units. But if S is not a census tract, then S intersects with a set of census tracts denoted as $\boldsymbol{y}$. The population of S is computed as:

$$\text{Pop}(S) = \sum_{y_x \in \boldsymbol{y}} \frac{\text{Area}\left(\text{Intersection}\left(S, y_x\right)\right)}{\text{Area}\left(y_x\right)} \cdot p_x \tag{2}$$

Let $\boldsymbol{v}$ be the set of Voronoi polygons intersected with spatial unit u, v_c be the Voronoi polygon and n_c be the footfall for cell tower c, the population-based method interpolates the footfall $n_{u,i=\text{Pop}}$ at a given spatial unit u proportional to the population, instead of to the total area:

$$n_{u,i=\text{Pop}} = \sum_{v_c \in \boldsymbol{v}} \frac{\text{Pop}\left(\text{Intersection}\left(u, v_c\right)\right)}{\text{Pop}\left(v_c\right)} \cdot n_c \tag{3}$$

Nevertheless, the population-based method has an important drawback since the population retrieved from the census will represent residential population rather that footfall, which might affect the way population dynamics in non residential areas are computed. Also, both uniform and population-based methods assume that the association of individuals to the closest cell tower location is always correct, which might not be the case specially for users who are at the boundaries of a given Voronoi polygon. Thus, researchers have used a third method to overcome this limitations, the inverse distance weighting (Idw) (Peredo et al. 2017; Ahas et al. 2015) that determines that the number of individuals in a spatial unit is the weighted average of its neighbor cellular towers where the weights are inversely proportional to the distance. The distance between a spatial unit and a cell tower is computed using their centroids. It is important to clarify that this method has only been used by researchers in combination with grids, not census tracts (Peredo et al. 2017; Ahas et al. 2015). Given $\boldsymbol{v}$ as the set of neighbor Voronoi polygons of spatial unit u, n_c as the footfall for cell tower c, and $d(u, v_c)$ as the distance between the centroids of u and v_c, the interpolated population for u is computed as follows:

$$n^*_{u,i=\text{Idw}} = \frac{\sum_{v_c \in \boldsymbol{v}} \frac{1}{d(u, v_c)} n_c}{\sum_{v_c \in \boldsymbol{v}} \frac{1}{d(u, v_c)}} \tag{4}$$

Let $\boldsymbol{s}^{(a,b)}$ be the set of spatial units and $\boldsymbol{v}^{(a,b)}$ be the set of Voronoi polygons intersecting with all spatial units in city a under boundary setting b. Interpolating using inverse distance weighting does not guarantee the sum of all $n^*_{u,a=\text{Idw}}$ for $u \in \boldsymbol{s}^{(a,b)}$ to be the same as the sum of all n_c for $v_c \in \boldsymbol{v}^{(a,b)}$. Therefore, we re-scale $n^*_{u,a=\text{Idw}}$ as follows:

$$n_{u,i=\text{Idw}} = n^*_{u,i=\text{Idw}} \frac{\sum_{v_c \in \boldsymbol{v}^{(a,b)}} n_c}{\sum_{u \in \boldsymbol{s}^{(a,b)}} n^*_{u,i=\text{Idw}}} \tag{5}$$

In summary, we consider in our paper the following combinations C of spatial units and interpolation methods: $(CT, Uni), (CT, Pop), (G, Uni), (G, Pop), (G, Idw), (Vor, Uni), (Vor, Pop)$, with grids of 500 x 500 meters, since this is one of the most common choices in the literature (Tu et al. 2017; Louail et al. 2014; Chen et al. 2018; Yang et al. 2016; Rubio et al. 2013). This is not meant to be a complete list of combinations. There are different types of spatial units and interpolation methods of interest. For example, one could take into account the terrain or land cover information to assign different relative population density (Scholz et al. 2013; Deville et al. 2014). Here we aim to analyze commonly

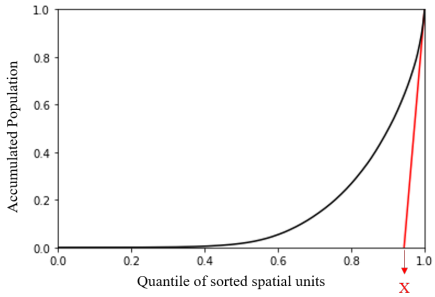

Figure 3. *Loubar* hotspot detection for a set of U spatial units with interpolated population. 1) the units are sorted in ascending order by the population; 2) draw the Lorenz curve of the accumulated population with x-axis being the ranking of units normalized by U; 3) compute the intersection of the tangent line at x=1.0 (the red line) and the x-axis. Let the intersection point be (X, 0); 4) The threshold δ is the population of the $U * (1 - X)$th spatial unit; 5) all spatial units with population $\geq \delta$ are the hotspots detected. The detailed explanation of *Loubar* method can be found in Louail et al. (2014).

used methods to shed light on potential stability issues. An example of the different spatial units and interpolation methods explored are shown in Step 2 in Figure 1.

Hotspot detection

To compute the hotspots of a city, we need to first identify the spatial units with a significant number of individuals. Hotspot detection is a binary classification problem, where the spatial units with a estimated number of people above a threshold value δ, *i.e.,* $n_u > \delta$, are considered as hotspots.

There exist different methods to determine the threshold δ (Hoteit et al. 2014; Giuliano and Small 1991). However, as previous work has shown, δ can be constrained within a lower and an upper bound (Louail et al. 2014). Given the estimated footfall for a set of spatial units, the lower bound of δ is defined as the average of the set of footfall values. On the other hand, the upper bound *i.e.,* the strictest definition of hotspot, is computed using the *Loubar* method based on the Lorenz curve. The *Loubar* method is briefly explained in Figure 3. In this paper, we will focus on the use of the upper bound, since it constitutes the strictest approach to measure the spatial structure of the most important places, and a result, strongest common denominator across different thresholds considered in the literature.

Given a CDR dataset, the *Loubar* method will be applied as follows. We will first aggregate the number of unique users for each cell tower c to obtain the average hourly number of unique users: $\overline{\boldsymbol{n}}_c = \{\overline{n}_{c,h}\}_{h=0}^{23}$, where $n_{c,h}$ represents the average of unique users between h:00:00 and h:59:59. Using equations (1) - (5), we can calculate the interpolated population with method i for a spatial unit u: $\overline{\boldsymbol{n}}_{u,i} = \{\overline{n}_{u,i,h}\}_{h=0}^{23}$.

Let $\boldsymbol{s}^{(a,b)}$ be all the spatial units in city a, $\boldsymbol{s}_m^{(a,b)}$ be the spatial units in a municipality m in city a in boundary setting b, and $\overline{\boldsymbol{N}}_{\boldsymbol{s},i,h} = \{\overline{n}_{u,i,h}\}_{u \in \boldsymbol{s}}$ be the interpolated population using method i for a set of spatial units $\boldsymbol{s}$ at hour h. We apply the *Loubar* hotspot detection method to $\overline{\boldsymbol{N}}_{\boldsymbol{s}^{(a,b)},i,h}$ if b is Metro-UR or Metro-U, or apply *Loubar* to $\overline{\boldsymbol{N}}_{\boldsymbol{s}_m^{(a,b)},i,h}$ for each municipality m in city a if b is PerMuni-UR or PerMuni-U to compute the threshold value δ and detect whether a spatial unit u is a hotspot at hour

h. Finally, a spatial unit will be identified as a hotspot if it is permanent *i.e.,* it is considered a hotspot throughout the 24 hours of the day (*all-day*) $\mathbb{1}_{u,i,h} = 1$ for $0 \leq h \leq 23$ (Louail et al. 2014). This binary decision can be denoted as:

$$\mathbb{1}_{u,i,h} = \begin{cases} 1, \text{if } \overline{n}_{u,i,h} \geq \delta \\ 0, \text{if } \overline{n}_{u,i,h} < \delta \end{cases} \tag{6}$$

However, since population density (Le Néchet 2012) and employment density (Giuliano and Small 1991) are often used in quantitative geography, which roughly correspond to the presence of people during nighttime and daytime, in this paper we will also explore *home-hour* and *work-hour* hotspots. These are formally defined as permanent hotspots during working hours (9am-5pm) or home hours (10pm-5am) *i.e.,* $1_{u,i,h} = 1$ for $h_s \leq h \leq h_e$ with $h_s = 9$ and $h_e = 17$ and with $h_s = 22$ and $h_e = 5$, respectively.

Hotspot measurement variables

In this paper, we will explore three types of hotspot measurement variables or *indices* that have been traditionally used in related literature for hotspot analyses at inter-city and intra-city levels: (1) scale of the hotspots, (2) degree of urban sprawl and (3) urban compactness. The first type quantifies the number of hotspots detected and the geographical area covered by them. The last two types of indices focus on the quantification of urban structure (Louail et al. 2014; Le Néchet 2012; Schwanen et al. 2001; Ewing 2008; Tsai 2005; Anas et al. 1998). Research in quantitative geography and urban economics has shown the importance of studying urban structure, as it can shape people's mobility in terms of travel distance, model choice and car usage (Schwanen et al. 2001; Le Néchet 2012), the transportation system in terms of energy consumption or air pollution (Le Néchet 2012; Ewing 2008), and economic growth performance (Xu et al. 2019; Huang et al. 2007). Next, we explain each set of indices in detail.

(1) Hotspot Scale quantified in terms of number and the total geographical area covered by the hotspots detected:

- Number of hotspots (NHS): The number of spatial units that are detected as hotspots.
- Area of hotspots (AHS): The total geographical area of the spatial units that are detected as hotspots.

(2) Urban sprawl represents a type of metropolitan decentralization or sub-urbanization where a large percentage of a city's residential and/or business activity takes place outside of its central location (Wassmer 2000). We use the following indices to quantify the degree of urban sprawl:

- Compacity coefficient (COMP) (Louail et al. 2014) measures the sprawl of the detected hotspots over a city, with smaller COMP values associated to less dispersed hotspots with respect to the size of the city. Let hs be the set of hotspots, $|hs|$ be the number of hotspots and $d_{j,k}$ the distance between the centroids of spatial units u_j and u_k, COMP is computed as Equation (7):

$$\text{COMP} = \frac{\text{D}_{hs}}{\sqrt{\text{Area}(r_{a,b})}}, \text{D}_{hs} = \frac{\sum_{j=1}^{|hs|} \sum_{k=j+1}^{|hs|} d_{j,k}}{|hs|\,(|hs|-1)/2} \tag{7}$$

- Mass Compacity coefficient (MCOMP) (Le Néchet 2012) is a modified compacity coefficient that weights the distance between hotspots by the population of each spatial unit, and measures the average distance between individuals located within the detected hotspots. The smaller MCOMP is, the less dispersed the hotspots are with respect to the size and population of the city. Let p_j be the population in spatial unit u_j, MCOMP is computed as follows:

$$\text{MCOMP} = \frac{\text{MD}_{hs}}{\sqrt{\text{Area}(r_{a,b})}}, \text{MD}_{hs} = \frac{\sum_{j=1}^{|hs|} \sum_{k=j+1}^{|hs|} d_{j,k}\, p_j\, p_k}{\sum_{j=1}^{|hs|} \sum_{k=j+1}^{|hs|} p_j\, p_k} \tag{8}$$

(3) Urban compactness is closely related to urban sprawl: the larger the degree of urban sprawl, the smaller the compactness of a city. However, one of the major differences between urban compactness and urban sprawl indices is that sprawl is always measured with respect to the size of a city *e.g.,* the indices are normalized by the square root of the geographical area, while compactness is based on the assumption that the most compact form of a shape is a circle (Angel et al. 2010). Therefore, compactness indices measure compactness in terms of geometrical properties, and are thus normalized by the reference circle, *e.g.,* an equal-area or equal-perimeter circle. Urban compactness indices range from 0 to 1, with 1 representing the exact continuous cirle. We consider the following four indices that are commonly used in hotspot measurement literature:

- Cohesion (COHE) (Angel et al. 2010) is the ratio of the average distance-squared among all points in the reference circle and the average distance-squared among all points in the hotspot areas. Large cohesion means people in hotspot areas are very close to each other.
- Proximity (PROX) (Angel et al. 2010) is the ratio of the average distance from all points in the reference circle to its centre and the average distance to the geometry center of the hotspot areas. The proximity index focuses on the distance between points from the geometry center instead of the point-wise distance in the cohesion index.
- Normalized moment of inertia (NMI) (Li et al. 2013) is based on the dispersion of points from the center of its shape. It involves the calculation of the second moment of an area about a point, also known as the moment of inertia (MI). The MI is then normalized by the MI of the reference circle, hence normalized moment of inertia. The calculation of NMI is explained in (Li et al. 2013).
- Normalized mass moment of inertia (NMMI) (Li et al. 2014) takes into account the mass distribution of a shape. The previous three compactness indices consider only the geometric shape *i.e.,* each point in the shape is equally important in the compactness. Nevertheless, in our case, each hotspot might have a different estimated population or mass, and they can still be compact - even though their geometry shape is not - by having the majority of the population concentrate around the mass center. The reference circle in NMMI is no longer an equal-area circle, but a circle with equal-effective-area. The calculation of NMMI is explained in Li et al. (2014).

Hotspot index stability

Hotspot indices are often used as a lens to study various aspects of urban life, and have been used to compare cities (inter-city analyses) (Louail et al. 2014; Ahas et al. 2015; Schwarz 2010; Huang et al. 2007), or to compare hourly hotspots within a city of interest (intra-city analyses) (Ratti et al. 2006; Reades et al. 2007; Kubíček et al. 2019; Tranos and Nijkamp 2015; Ahas et al. 2015). For example,

research has shown that high density cities in the UK share higher levels of public transportation use by low-income residents (Burton 2000); while other studies have revealed that hotspot compactness has a significant negative correlation with purchasing power parity in cities in Asia, US, Europe, Latin America and Australia (Huang et al. 2007).

Nevertheless, the choice of city boundaries, spatial units and interpolation methods prior to the computation of hotspots and hotspot indices could produce significant differences in the hotspots identified, which could in turn provide conflicting findings. For example, a researcher interested in using hotspots to predict crime in a city, could find a strong correlation or no correlation at all, depending on the set of city boundaries, spatial units and interpolation methods as well as hotspot variables considered; or a researcher interested in comparing number of hotspots across cities, could identify largely different city-rankings depending on the sets of features used.

The main objective of this paper is to provide a systematic analysis of the impact that the choice of a given set of city boundaries, types of spatial units and interpolation methods might have on the stability of the hotspot indices presented. The recommendations of these analyses will provide guidelines for researchers looking to identify the combination of parameters that will preserve the stability of the hotspot indices; and will pinpoint into risky combinations of features that might produce hotspot indices with little stability. Next, we explain our approach to measuring the stability of a hotspot index for both inter-city and intra-city scales.

Inter-city Index Stability. Inter-city analyses focus on comparing rankings of cities based on a given hotspot index, or on comparing rankings of cities based on correlations between a given hotspot index and another urban feature such as crime or economic growth. Thus, to measure the stability of a given inter-city index, we propose the following approach. For each combination of city boundary b, type of spatial unit t (Vor, G or CT) and interpolation method i (Uni, Pop or Idw), we compute the hotspots and hotspot indices described in the methodology section across all cities under study. Next, we conduct Spearman correlation for each pair of city rankings resulting from different combinations of features, and compute the stability of an index for a given citye boundary, as the average of all correlation coefficients across spatial units and interpolation methods. High average correlation coefficients across combinations of features will reveal that the hotspot index is stable *i.e.,* the ranking of the cities for a given index is similar independently of the spatial features used. Researchers could select any set of features since the rankings do not appear to change, and as result, any correlation analyses between hotspots and other features would also be robust. On the other hand, low average correlation coefficients will identify indices that should not be used since the rankings vary widely depending on the combination of features.

Let $\boldsymbol{C} = \{(CT, Uni), (CT, Pop), (G, Uni), (G, Pop), (G, Idw), (Vor, Uni), (Vor, Pop)\}$ be the list of combinations of type t spatial units and interpolation method i considered in this study, with $|\boldsymbol{C}|$ as the number of combinations and C_j as the j-th combination where $1 \leq j \leq |C|$. For each hotspot index $ind \in \{$NHS, AHS, COMP, MCOMP, COHE, PROX, NMI, NMMI$\}$, city boundary b and combination $C_j = (t_j, i_j)$, we first compute the permanent hotspots (all-day/work-hour/home-hour) and then compute the index values for all cities under study. Each combination C_j will produce an array of index values, one per city, defined as $\boldsymbol{ind}_{b,C_j}$. Next, for each pair of combinations C_j and C_k, we compute the correlation coefficient for index ind and city boundary b as:

$$Coef_{ind,b,j,k} = \text{Spearman}(\boldsymbol{ind}_{b,C_j}, \boldsymbol{ind}_{b,C_k}) \tag{9}$$

The coefficient measures the similarity of rankings among cities. Then the stability for index ind and city boundary b is computed as:

$$Stability_{ind,b} = \frac{1}{|\boldsymbol{C}|\,(|\boldsymbol{C}|-\mathbf{1})} \sum_{j,k \leq |C|,\, j \neq k} Coef_{ind,b,j,k} \tag{10}$$

Intra-city Index Stability. Intra-city analyses generally focus on comparing hotspot rankings across time for a given city. Index stability at the intra-city level is helpful to identify the indices that provide similar hourly rankings independently of the spatial and interpolation features used. Stable indices can thus be used to robustly study the relationship between hotspots and urban growth or transportation efficiency, for example; while unstable indices will be discouraged from use given the variability of the rankings they provide. To measure the stability of an index at the intra-city level, given a city a defined using an city boundary setting b, we first compute the hotspots at each hour h using combination $C_j = (t_j, i_j)$. This yields a 24-hour vector $\boldsymbol{ind}_{b,C_j,a}$ for each combination C_j and city a. Pairs of combinations C_j and C_k are compared in terms of ranking similarity in city a via Spearman correlation.

$$Coef_{ind,b,a,j,k} = \text{Spearman}(\boldsymbol{ind}_{b,C_j,a}, \boldsymbol{ind}_{b,C_k,a}) \tag{11}$$

The intra-city level stability for index ind at city a using city boundary b is the computed as:

$$Stability_{ind,b,a} = \frac{1}{|\boldsymbol{C}|\,(|\boldsymbol{C}|-\mathbf{1})} \sum_{j,k \leq |C|,\, j \neq k} Coef_{ind,b,a,j,k} \tag{12}$$

Finally, to identify the stability of a given index for a certain city boundary and spatial combination, we average the stability measure across all the cities $a \in A$ under study:

$$Stability_{ind,b} = \frac{1}{A} \sum_{a=1}^{A} Stability_{ind,b,a} \tag{13}$$

Spearman correlation coefficients will be interpreted as follows (Statstutor 2020): a stability score in range of $[0.8, 1)$ is considered very strongly stable; in range of $[0.6, 0.8)$ is considered strongly stable; moderately stable in the $[0.4, 0.6)$ range; weakly stable in the range of $[0.2, 0.4)$ and unstable in the $[0.0, 0.2)$ range.

Results

Study areas and Dataset

To carry out our analyses, we use pseudonymised CDR data from the 59 top metropolitan areas in Mexico (see Figure 4). The data covers cell phone activity from October 2009 to June 2010. No individual data has been used, only aggregated statistics at the cell tower level to quantify the number of unique users per hour. City boundaries have been defined using official shapefiles for metropolitan areas as defined by CONAPO, the National Population Council in Mexico (CONAPO 2015). Municipalities, census tracts (known as AGEBs in Mexico) and urban and rural areas have been extracted from INEGI, the statistical department in Mexico (INEGI 2010), with data from 2010.

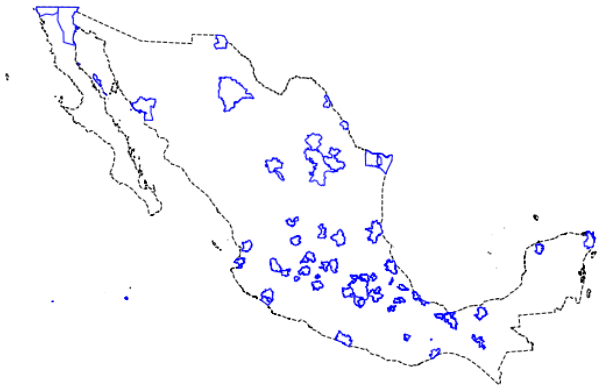

Figure 4. 59 metropolitan areas in Mexico

	Metro UR	Metro U	PerMuni UR	PerMuni U
NHS	0.39 (0.31)	0.61 (0.17)	0.65 (0.16)	0.76 (0.09)
AHS	0.33 (0.24)	0.64 (0.17)	0.55 (0.17)	0.81 (0.06)
COMP	0.55 (0.17)	0.61 (0.16)	0.71 (0.17)	0.77 (0.08)
MCOMP	0.56 (0.16)	0.61 (0.16)	0.72 (0.11)	0.73 (0.10)
COHE	0.40 (0.19)	0.53 (0.10)	0.49 (0.17)	0.64 (0.11)
PROX	0.40 (0.19)	0.53 (0.13)	0.50 (0.17)	0.62 (0.11)
NMI	0.40 (0.19)	0.53 (0.10)	0.52 (0.15)	0.64 (0.11)
NMMI	0.41 (0.17)	0.53 (0.11)	0.57 (0.11)	0.62 (0.14)

(a) All-day

	Metro UR	Metro U	PerMuni UR	PerMuni U
NHS	0.52 (0.28)	0.74 (0.12)	0.65 (0.18)	0.80 (0.09)
AHS	0.46 (0.22)	0.76 (0.12)	0.58 (0.16)	0.86 (0.05)
COMP	0.57 (0.14)	0.68 (0.13)	0.70 (0.19)	0.78 (0.10)
MCOMP	0.59 (0.15)	0.63 (0.16)	0.73 (0.11)	0.73 (0.10)
COHE	0.41 (0.19)	0.55 (0.11)	0.44 (0.19)	0.67 (0.12)
PROX	0.41 (0.19)	0.53 (0.13)	0.45 (0.19)	0.65 (0.13)
NMI	0.41 (0.19)	0.55 (0.11)	0.47 (0.17)	0.67 (0.12)
NMMI	0.43 (0.19)	0.55 (0.13)	0.59 (0.12)	0.65 (0.15)

(b) Work-hour

	Metro UR	Metro U	PerMuni UR	PerMuni U
NHS	0.42 (0.30)	0.68 (0.14)	0.67 (0.15)	0.80 (0.08)
AHS	0.37 (0.24)	0.73 (0.14)	0.57 (0.16)	0.85 (0.05)
COMP	0.58 (0.15)	0.64 (0.15)	0.72 (0.16)	0.78 (0.08)
MCOMP	0.59 (0.14)	0.68 (0.12)	0.74 (0.11)	0.73 (0.13)
COHE	0.35 (0.22)	0.53 (0.11)	0.46 (0.19)	0.65 (0.11)
PROX	0.37 (0.22)	0.54 (0.13)	0.47 (0.18)	0.63 (0.11)
NMI	0.35 (0.22)	0.53 (0.11)	0.48 (0.16)	0.65 (0.11)
NMMI	0.42 (0.19)	0.55 (0.11)	0.56 (0.12)	0.64 (0.14)

(c) Home-hour

Figure 5. Stability (Standard deviation) of all indices in different boundary settings. The gradient background color is based on the stability score ranging from 0 to 1, the darker the orange color is, the closer it is to 1.

Inter-city level analysis

Figure 5 shows the stability scores for each hotspot index and city boundary, with each table representing all-day, work-hour and home-hour hotspots. Recall that each stability value is computed as the average of all Spearman correlations between all pairs of combinations of spatial units and interpolation methods. To measure that variance, each table also shows the standard deviation of the stability in parentheses. Next, we describe the main outcomes, followed by an in-depth discussion in the next section. Based on the Figure, we observe:

1) All hotspot indices are the most stable when cities are defined by their urban municipalities only (PerMuni-U) with average correlations between different spatial unit and interpolation combinations ranging from 0.62 to 0.86 - very strongly correlated - across methods. Hotspot indices are least stable when cities are defined by their metropolitan area and considering both urban and rural regions (Metro-UR, with stability values from 0.33 to 0.59). Generally, it is fair to say that all indices tend to be more stable in settings that consider only urban areas and independent municipalities, rather than

	CT Uni	CT Pop	G Idw	G Uni	G Pop	Vor Uni	Vor Pop	Mean
CT Uni	1.00	0.55	0.47	0.50	0.65	0.15	0.23	0.43
CT Pop	0.55	1.00	0.40	0.49	0.68	0.30	0.31	0.45
G Idw	0.47	0.40	1.00	0.31	0.53	0.32	0.40	0.41
G Uni	0.50	0.49	0.31	1.00	0.57	0.18	0.06	0.35
G Pop	0.65	0.68	0.53	0.57	1.00	0.20	0.31	0.49
Vor Uni	0.15	0.30	0.32	0.18	0.20	1.00	0.80	0.32
Vor Pop	0.23	0.31	0.40	0.06	0.31	0.80	1.00	0.35

Figure 6. Spearman correlation coefficient $Coef_{ind=PROX,b=Metro\text{-}UR,j,k}$ between each pair of combinations (C_j, C_k) for all-day permanent hotspots. The coefficient matrix is symmetric. The row mean is the average of coefficients in each row, excluding the values on the diagonal. The row mean of j-th row shows the average coefficients of combination C_j correlated with other combinations.

whole metropolitan areas. As a result, and whenever possible, city boundaries that consider only urban municipalities should be favored in inter-city analyses since the ranking of cities will likely remain stable and comparisons with other urban features - *e.g.,* crime - will be robust thus avoiding conflicting results.

2) Scale of hotspot indices (NHS, AHS) and urban sprawl indices (COMP, MCOMP) are the most stable. For 3 out of 4 city boundary settings, NHS, COMP and MCOMP are between strongly and very strongly stable. Therefore, compared to the compactness indices, researchers have more freedom to choose the boundary settings and interpolation methods for inter-city level comparisons that are based on scale of hotspots and degree of urban sprawl. This means that under the same city boundary setting, comparison among cities in terms of these two indices or correlation with other factors using them are less likely to produce conflicting findings across combinations of types of spatial units and interpolation methods. Finding (1) revealed that PerMuni-U produces the most stable indices across types. However, the second most stable boundary setting for scale of hotspots and urban sprawl is different. Scale of hotspots' second best setting is Metro-U while for urban sprawl is PerMuni-UR. For urban sprawl, the difference between the stability in PerMuni-UR and in PerMuni-U is small. Therefore, as long as researchers are using PerMuni-based settings, whether or not to include rural areas does not have a large impact in terms of stability.

3) Compactness indices (COHE, PROX, NMI and NMMI) are the least stable indices. When making comparisons at the inter-city level in terms of compactness indices, researchers should first pay attention to the boundary settings because compactness indices are strongly stable only in the PerMuni-U setting and moderate to weakly stable in the other three settings. When PerMuni-U setting is undesired, *e.g.,* rural areas need to be incorporated, our proposed method allows researchers to explore in depth the relationship between spatial units, interpolation methods and stability for a selected city boundary; to then choose the most stable combination within the unstable setting. For example, Figure 6 shows the Spearman correlations among the different combinations for the PROX index in the Metro-UR boundary setting. We can observe that, in general, the stability across all combinations is low. However, if researchers need to use a Metro-based setting, the (G, Pop) combination tends to have the largest average correlations (0.49) and thus, the largest stability which would make it the top candidate combination to use when extracting hotspots at both urban and rural scales. Similar results are observed for COHE, NMI and NMMI.

	Metro UR	Metro U	PerMuni UR	PerMuni U
NHS	0.38 (0.17)	0.38 (0.17)	0.31 (0.12)	0.35 (0.17)
AHS	0.43 (0.18)	0.41 (0.19)	0.36 (0.16)	0.39 (0.18)
COMP	0.52 (0.23)	0.52 (0.24)	0.30 (0.13)	0.33 (0.14)
MCOMP	0.49 (0.22)	0.49 (0.24)	0.36 (0.19)	0.40 (0.21)
COHE	0.25 (0.10)	0.29 (0.11)	0.29 (0.15)	0.35 (0.16)
PROX	0.26 (0.11)	0.30 (0.12)	0.29 (0.15)	0.35 (0.17)
NMI	0.25 (0.10)	0.29 (0.11)	0.29 (0.15)	0.35 (0.16)
NMMI	0.30 (0.11)	0.33 (0.14)	0.35 (0.15)	0.39 (0.15)

(a) 24-hour vector

	Metro UR	Metro U	PerMuni UR	PerMuni U
NHS	0.40 (0.14)	0.42 (0.15)	0.40 (0.16)	0.43 (0.18)
AHS	0.39 (0.15)	0.42 (0.16)	0.34 (0.14)	0.41 (0.17)
COMP	0.48 (0.21)	0.49 (0.23)	0.30 (0.12)	0.36 (0.15)
MCOMP	0.46 (0.22)	0.47 (0.23)	0.39 (0.18)	0.41 (0.22)
COHE	0.32 (0.14)	0.35 (0.14)	0.32 (0.16)	0.37 (0.16)
PROX	0.33 (0.15)	0.37 (0.15)	0.32 (0.17)	0.38 (0.16)
NMI	0.32 (0.14)	0.35 (0.14)	0.32 (0.16)	0.37 (0.16)
NMMI	0.37 (0.15)	0.39 (0.17)	0.39 (0.17)	0.44 (0.16)

(b) 4-hour-bin vector

Figure 7. Stability (Standard deviation) of all indices in different boundary settings. The coefficients in (a) are computed using 24-hour vector of indices and in (b) are computed using 4-hour-bin vector. The gradient background color is based on the stability score ranging from 0 to 1, the darker the orange color is, the closer it is to 1.

4) In most cases, the stability for different indices and boundary settings is similar among all-day, work-hour and home-hour permanent hotspots. But the home-hour stability in Metro-UR settings for COHE, PROX and NMI is consistently smaller than all-day and work-hour.

Intra-city level analysis

The stability scores at the intra-city level for each hotspot index and across boundary settings are shown in Figure 7(a). Standard deviation values for each stability score - representing the spread of the correlations among different combinations of spatial units and interpolation methods - are also shown. From the Figure, we can observe that:

1) Hotspot scale and urban sprawl indices are more stable in Metro-based settings, while urban compactness indices highest stability is achieved when using municipalities to define city boundaries. Nevertheless, the impact of boundary settings is small for urban compactness indices. Based on these findings, researchers could favour one type of indices versus others depending on the boundary settings of interest, which would in turn produce more robust indices to measure hotspot rankings over time for a given city.

2) The highest stability score is achieved by urban sprawl indices (COMP and MCOMP) under Metro-UR and Metro-U boundary settings. This is different from the inter-city level stability analyses where the best score was achieved with PerMuni-based settings. However, even the highest stability is only moderately stable. AHS also has moderate stability under Metro-UR and Metro-U boundary settings. The rest indices in all settings are weakly stable, much lower than the stability scores at the inter-city level, indicating that a change in the boundary or spatial unit choice could produce widely different results.

3) The intra-city stability scores per index are computed extracting permanent hourly hotspots *i.e.,* hotspots that are considered as such throughout the 24 hours. As a result, the low stability scores could be potentially due to the stringent definition of hotspot. To assess that, we grouped the 24 hours into 6 bins - each bin is a 4-hour-bin - and computed the hotspot indices again. In this case, the Spearman correlation was computed between two 6-bin vectors of coefficients - instead of the previous 24-hour

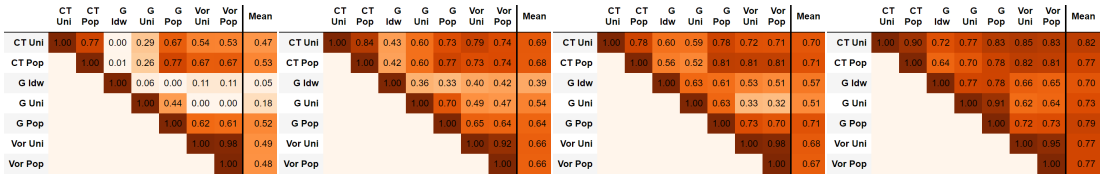

(a) Metro-UR setting (b) Metro-U setting (c) PerMuni-UR setting (d) PerMuni-U setting

Figure 8. Spearman correlation coefficients $Coef_{ind=NHS,b,j,k}$ between each pair of combinations (C_j,C_k) under four different boundary settings. The coefficient matrix is symmetric whose lower triangular part is omitted.

vectors. Figure 7(b) shows that although the stability scores increase, except for the COMP index in the Metro-based setting, they are still mostly weakly stable.

Finally, it is important to mention that although the index stability scores at the intra-city scale are on average low, some cities do have much higher stability scores than others. This finding might be indicating that, unlike inter-city scales, intra-city hotspots' stability might depend on other types of cultural or social trends not studied in this paper.

Discussion

In this section, we explore potential reasons behind the stability findings described in the previous section.

Stability of hotspot scale indices (NHS and AHS) at the inter-city level

As explained in the previous section, hotspot scale indices (NHS and AHS) are more stable when city boundaries are defined using only urban municipalities. We posit that this might be due to the fact that rural areas, which generally have smaller footfall, are dramatically changing the Lorenz curves and, as a result, the scale of the hotspots computed. We will now analyze in depth a few case examples that are representative of the global trends observed in our analyses. Figure 8(a) shows the Spearman correlation coefficients for the NHS index across all the combinations of spatial unit and interpolation methods per each of the four boundary settings. We can observe that combinations (*G, Uni*) and (*G, Idw*) are weakly or even not correlated with other methods in the *Metro-UR* causing the low stability score. Changing to other boundary settings, such as excluding the rural areas, all the coefficients involving methods (*G, Uni*) and (*G, Idw*) have a large increase and as a result NHS becomes more stable in *Metro-U* setting. Therefore, we will compare the NHS computed based on combinations *(G, Idw)* and *(G, Pop)* to explore what might cause the unstability or dissimilarity in the cities ranking.

Figure 9(a) and 9(b) shows the comparison between Metro-UR and Metro-U settings for city 34 (Puebla-Tlaxcala Metropolitan Area) and city 39 (Rioverde-Ciudad Fernández Metropolitan Area). Each plot represents the Lorenz curve used to compute NHS_a based on a combination $C = (t, i)$ of type of spatial units t and interpolation method i in city a. We can observe that the more rural areas a city has, the more heavily the shape of Lorenz curve is changed by different combinations C, which causes variations in the number of hotspots identified. For example, Figure 9(a) shows that under the Metro-UR setting, $\text{NHS}_{34} = 200$ and for $\text{NHS}_{39} = 34$ based on the combination *(G, Pop)*, which means that the ranking of

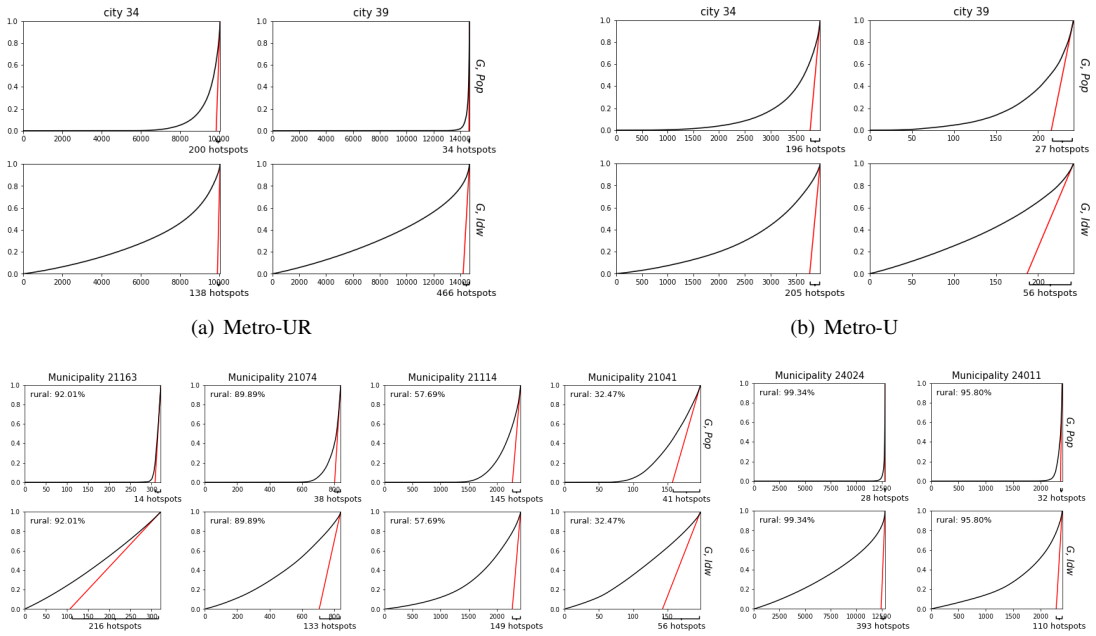

(a) Metro-UR

(b) Metro-U

(c) PerMuni-UR, municipaliites in city 34

(d) PerMuni-UR, municipaliites in city 39

Figure 9. Lonrenz curves for loubar-based hotspots detection in city 34 and 39 in different boundary settings. The x-axis is rescaled to the number of spatial units to better explain the difference in NHS. Combination *(G, Pop)* and *(G, Idw)* are shown for comparison. City 34 has 70% of rural areas and 39 municipalities with various percentage of rural areas while city 39 has 99% of rural areas and 2 municipalities both with more than 95% of rural areas.

city 34 is higher than 39. Changing to the combination *(G, Idw)*, NHS_{34} decreases to 138 but NHS_{39} increases to 466 showing that the ranking of cities 34 and 39 has reversed. This is caused by the fact that city 39 has more rural areas (99%) than city 34 (70%), and the Lorenz curve for city 39 is impacted more (much more closer to the diagonal) by changing from *(G, Pop)* to *(G, Idw)* than the curve for city 34.

On the other hand, the spatial units in the rural areas are not considered in the hotspots detection under the Metro-U setting. For example, the number of grids considered in city 39 in Metro-U setting is about 250, much smaller than in Metro-UR setting which is about $14,500$. The impact brought by the variation in percentage of rural areas is mitigated by focusing on urban areas only in the Metro-U setting *i.e.,* the change in the Lonrenz curve and change in NHS from *(G, Pop)* to *(G,Idw)* is smaller and more consistent in both cities. Changing from *(G, Pop)* to the *(G, Idw)*, NHS_{34} increases from 196 to 205 and NHS_{39} increases from 27 to 56. Therefore the ranking of both cities are better preserved between these two combinations.

Next, we shift our focus to the Permuni-UR setting. In PerMuni-based settings hotspots are detected per municipality. Therefore, the Lorenz curves might be affected by the percentage of rural areas in each municipality. City 34 as a whole metropolitan area has 70% rural areas, but it has 39 municipalities with

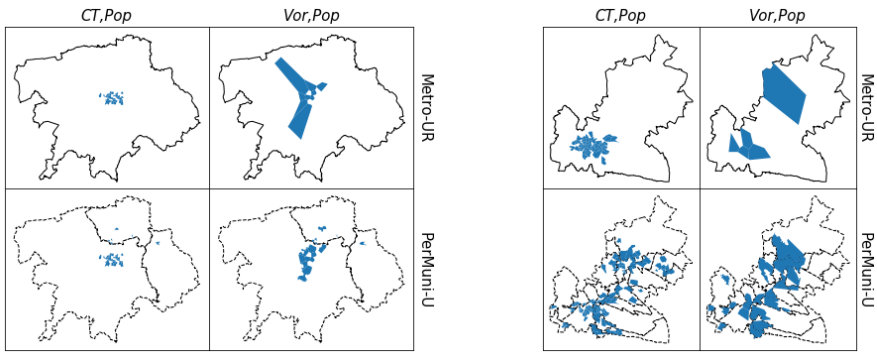

(a) city 25 (b) city 46

Figure 10. Permanent hotspots detected by combinations *(CT, Uni) (Vor, Pop)* for city 25 and 46.

various percentages of rural areas from 1% to 92%. Four example municipalities are shown in Figure 9(c). City 39 has 2 municipalities, both of which have similar percentages of rural areas as city 39 as a whole, shown in Figure 9(d). We observe that for municipalities with high percentage of rural areas *e.g.,* municipality 22163, 21074, 24024, 24011 in Figure 9(c) and 9(d), the Lorenz curves are also heavily impacted by changing from *(G, Pop)* to *(G, Idw)*. For municipalities with lower percentage of rural areas *e.g.,* municipality 21114, 21041 in Figure 9(c), the Lorenz curves are less impacted. As a result, changing from *(G, Pop)* to *(G, Idw)*, the NHS_{34} changes from 905 to 3663 and the NHS_{39} changes from 60 to 503. Although city 34 still has a smaller change in NHS (increased 3 times) than city 39 (increased 7.4 times), the ranking between them is preserved. Therefore the stability of NHS in Permuni-UR is better than in Metro-UR.

Stability of urban sprawl indices (COMP and MCOMP) at the inter-city level

As discussed in the previous section, urban sprawl indices computed with PerMuni-based boundary settings appear to be more stable than Metro-based ones. One of the possible reasons might be the different ways in which the population of a metropolitan area can be distributed across municipalities. For example, some metropolitan areas have a dominant urban core with the majority of human activities, while in other metropolitan areas there might be municipalities acting as sub-centers with similar levels of activity as their urban cores.

Take city 25 (Morelia Metropolitan Area) and 46 (Tlaxcala-Apizaco Metropolitan Area) as examples (Figure 10). Both city 25 and 46 have multiple municipalities and each municipality has an urban area. But in city 25, the urban core is dominating, that is, the population of city 25 is mostly concentrated in one core urban region *e.g., (CT, Pop)* and *(Vor, Pop)* in Metro-UR setting in Figure 10(a). While in city 46, the location of the hotspots varies. With the combination *(CT, Pop)* in Metro-UR, the permanent hotspots concentrate in the left-bottom corner (Figure 10(b)), just like city 25. But with the combination *(Vor, Pop)* in Metro-UR, permanent hotspots in other municipalities are detected thus increasing the value of the COMP index (Figure 10(b)). As a result, since different metropolitan areas have different

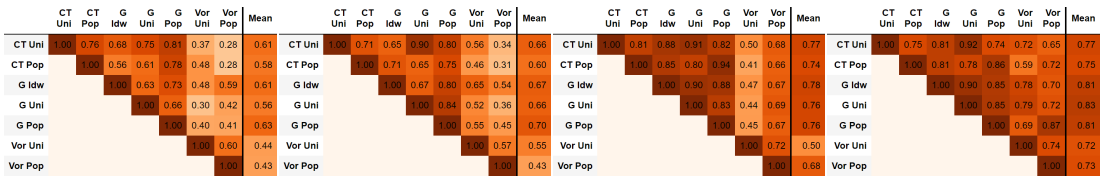

(a) Metro-UR setting (b) Metro-U setting (c) PerMuni-UR setting (d) PerMuni-U setting

Figure 11. Spearman correlation coefficient $Coef_{ind=COMP,b,j,k}$ between each pair of between each pair of combinations (C_j,C_k) under four boundary settings. The coefficient matrix is symmetric whose lower triangular part is omitted.

distributions of population over multiple municipalities, hotspots indices computed over metropolitan-based settings are not as stable. On the other hand, detecting hotspots in the municipality-based settings is more stable because the permanent hotspots are local to each municipality and overall the hotspots spread over multiple municipalities (see the second row in Figure 10(a) and 10(b)). And because COMP is normalized by the square-root of city's geographical area, the distance between hotspots spreading over the city is normalized. Therefore variances in the population distribution bring less instability to COMP indices across spatial units and interpolation methods.

Rural areas also appear to play a role in index stability. Figure 11 shows the correlation coefficients for each pair of spatial unit and interpolation method combination across all boundary settings for the COMP index. We can observe that combinations *(Vor, Uni)* and *(Vor, Pop)* are the least correlated with other combinations, especially in settings including rural areas. When considering rural areas, the Voronoi polygons can cover large regions *e.g.,* the plot of *(Vor, Pop)* using the Metro-UR setting in Figure 10(a) and 10(b), as the cell towers tend to be sparse in rural areas. Since urban sprawl indices are computed based on the distance among centroids of polygons, these large Voronoi polygons drag the centroids away from dense population areas; and since the sizes of the Voronoi polygons are not homogeneous across different metropolitan areas, the inclusion of rural areas brings in high instability to hotspot urban sprwal indices.

Stability of urban compactness indices (COHE, PROX, NMI and NMMI) at the inter-city level

Urban compactness indices, similarly to urban sprawl, are computed using the distance between the detected hotspots. Therefore, these indices are subject to the same instability issues due to the various ways in which population and footfall can be distributed across municipalities, and to the varying shapes that Voronoi polygons might have in rural areas. Comparing Figures 11 and 12 we can also observe that the correlation between *Vor*-based and other spatial combinations is much worse for urban compactness indices than for urban sprawl indices. This is because compactness indices measure the compactness of the shape of hotspots, and the varying nature of the Voronoi polygons causes the *Vor*-based combinations to be weakly to no correlated with other combinations when the rural areas are considered.

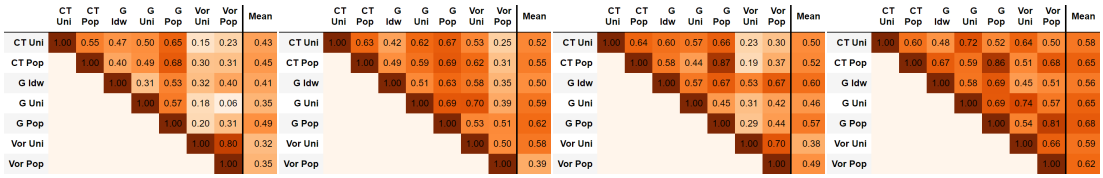

(a) Metro-UR setting (b) Metro-U setting (c) PerMuni-UR setting (d) PerMuni-U setting

Figure 12. Spearman correlation coefficient $Coef_{ind=PROX,b,j,k}$ between each pair of between each pair of combinations (C_j,C_k) under four boundary settings. The coefficient matrix is symmetric whose lower triangular part is omitted.

Difference of stability between home-hour and work-hour permanent hotspots at inter-city level

There exists little difference in the stability of hotspot indices computed for home- and work-hour periods across different city boundary settings. Nevertheless, it is worth noting that the stability scores for COHE, PROX and NMI computed for home-hour periods are slightly more unstable than their work-hour counterpart, especially in the Metro-UR setting. We argue that this might be due to the fact that for some cities home locations are more spatially scattered, possibly including the outskirts where CT and Vor polygons tend to be larger when compared to work locations in downtown areas that tend to have smaller CT and Voronoi polygons. Thus, these varying area sizes in home location polygons might be increasing the instability of the indices. See Figure 13 for an example of this setting with city 10 (Tuxtla Gutiérrez Metropolitan Area), city 30 (Tepic Metropolitan Area) and city 32 (Oaxaca Metropolitan Area). The home-hour permanent hotspots are more scattered than the work-hour permanent hotspots. Using *(G, Pop)*, a few small grids away from the core area in city 30 and 32 are considered as permanent hotspots. But using *(Vor, Pop)*, the Voronoi polygons away from the core area have large variation in size. The variation in size would have a huge impact on the covered geographic area and subsequently on the equal-area circle considered in the compactness indices. Therefore, COHE, PROX and NMI have slightly lower stability in home-hour period.

Conclusions

The rich spatio-temporal information provided by CDR data has provided great potential for studying human mobility dynamics in urban environments. A bulk of the literature has used CDR data to study the relationship between human dynamics - modelled through hotspot areas in cities - and various urban characteristics, such as spatial structure, transportation efficiency and energy consumption. However, most of these studies are based on ad-hoc selections of city boundaries and spatial units.

In this paper, we conduct a systematic analysis of the stability of various hotspot indices at both inter-city and intra-city levels. We have found that at the inter-city level, the urban municipality boundary is the best setting to obtain stable and robust city ranking results. Indices for scale of hotspots and degree of urban sprawl are strongly stable across all city boundary settings. Therefore, when a particular city boundary setting is desired, NHS, AHS, COMP and MCOMP are good indices to work with. If the compactness family of indices (COHE, PROX, NMI and NMMI) are of interest, it is better to use the

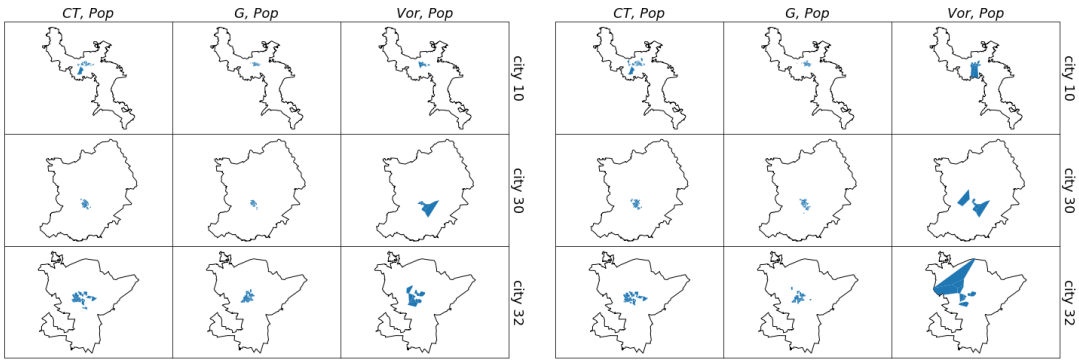

(a) Work-hour permanent hotspots

(b) Home-hour permanent hotspots

Figure 13. Permanent hotspots detected by methods *(CT, Pop)*, *(G, Pop)*, *(Vor, Pop)* for city 10, city 30 and city 32 in work and home hours under boundary setting b=Metro-UR

municipalities with urban and rural areas (PerMuni-UR setting). If other city boundaries are required, we recommend using the (G, Pop) interpolating method as this method tends to be most correlated with other methods in all settings.

For intra-city level, the stability of indices are mostly weakly stable. Only the degree of urban sprawl (COMP and MCOMP) in Metro-based settings have moderate stability. The stability of indices in different cities has large variation, meaning some indices can be very strongly stable across interpolation methods in some cities but not stable at all in other cities. We have not find any index or boundary setting that would work well across cities. Thus it is vital for researchers to use consistent type of spatial units and interpolation methods. We also intend to explore the characteristics of cities that contribute the stability of indices in the future work.

Declaration of conflicting interests

The author(s) declared no potential conflicts of interest with respect to the research, authorship, and/or publication of this article.

References

Ahas R, Aasa A, Yuan Y, Raubal M, Smoreda Z, Liu Y, Ziemlicki C, Tiru M and Zook M (2015) Everyday space–time geographies: using mobile phone-based sensor data to monitor urban activity in harbin, paris, and tallinn. *Int. J. Geogr. Inf. Sci.* 29(11): 2017–2039. DOI:10.1080/13658816.2015.1063151.

Anas A, Arnott R and Small KA (1998) Urban spatial structure. *J. Econ. Lit.* 36(3): 1426–1464.

Angel S, Parent J and Civco DL (2010) Ten compactness properties of circles: measuring shape in geography. *The Canadian Geographer / Le Géographe canadien* 54(4): 441–461. DOI:10.1111/j.1541-0064.2009.00304.x.

Bachir D, Gauthier V, Yacoubi ME and Khodabandelou G (2017) Using mobile phone data analysis for the estimation of daily urban dynamics. In: *2017 IEEE 20th International Conference on Intelligent Transportation Systems (ITSC)*. pp. 626–632. DOI:10.1109/ITSC.2017.8317956.

Balzotti C, Bragagnini A, Briani M and Cristiani E (2018) Understanding human mobility flows from aggregated mobile phone data. *IFAC-PapersOnLine* 51(9): 25–30.

Becker RA, Caceres R, Hanson K, Loh JM, Urbanek S, Varshavsky A and Volinsky C (2011) A tale of one city: Using cellular network data for urban planning. *IEEE Pervasive Comput.* 10(4): 18–26. DOI:10.1109/MPRV.2011.44.

Bogomolov A, Lepri B, Staiano J, Letouzé E, Oliver N, Pianesi F and Pentland A (2015) Moves on the street: Classifying crime hotspots using aggregated anonymized data on people dynamics. *Big data* 3(3): 148–158.

Burton E (2000) The compact city: Just or just compact? a preliminary analysis. *Urban Stud.* 37(11): 1969–2006. DOI:10.1080/00420980050162184.

Calabrese F, Colonna M, Lovisolo P, Parata D and Ratti C (2011) Real-Time urban monitoring using cell phones: A case study in rome. *IEEE Trans. Intell. Transp. Syst.* 12(1): 141–151. DOI:10.1109/TITS.2010.2074196.

Candia J, González MC, Wang P, Schoenharl T, Madey G and Barabási AL (2008) Uncovering individual and collective human dynamics from mobile phone records. *J. Phys. A: Math. Theor.* 41(22): 224015. DOI: 10.1088/1751-8113/41/22/224015.

Chen J, Pei T, Shaw SL, Lu F, Li M, Cheng S, Liu X and Zhang H (2018) Fine-grained prediction of urban population using mobile phone location data. *Int. J. Geogr. Inf. Sci.* 32(9): 1770–1786. DOI:10.1080/13658816.2018.1460753.

CONAPO (2015) DelimitaciÓn de zonas metropolitanas. `http://www.conapo.gob.mx/es/CONAPO/Datos_Abiertos_Delimitacion_de_Zonas_Metropolitanas`. Accessed: 2020-01-17.

Demographia (2020) Definition of urban terms. `http://demographia.com/db-define.pdf`. Accessed: 2020-01-17.

Deville P, Linard C, Martin S, Gilbert M, Stevens FR, Gaughan AE, Blondel VD and Tatem AJ (2014) Dynamic population mapping using mobile phone data. *Proc. Natl. Acad. Sci. U. S. A.* 111(45): 15888–15893. DOI: 10.1073/pnas.1408439111.

Dong Y, Pinelli F, Gkoufas Y, Nabi Z, Calabrese F and Chawla NV (2015) Inferring unusual crowd events from mobile phone call detail records. In: *Machine Learning and Knowledge Discovery in Databases*. Springer International Publishing, pp. 474–492. DOI:10.1007/978-3-319-23525-7_29.

Douglass RW, Meyer DA, Ram M, Rideout D and Song D (2015) High resolution population estimates from telecommunications data. *EPJ Data Science* 4(1): 4. DOI:10.1140/epjds/s13688-015-0040-6.

Doyle J, Hung P, Farrell R and McLoone S (2014) Population mobility dynamics estimated from mobile telephony data. *Journal of Urban Technology* 21(2): 109–132. DOI:10.1080/10630732.2014.888904.

Ewing RH (2008) Characteristics, causes, and effects of sprawl: A literature review. In: Marzluff JM, Shulenberger E, Endlicher W, Alberti M, Bradley G, Ryan C, Simon U and ZumBrunnen C (eds.) *Urban Ecology: An International Perspective on the Interaction Between Humans and Nature*. Boston, MA: Springer US. ISBN 9780387734125, pp. 519–535. DOI:10.1007/978-0-387-73412-5_34.

Fryer RG and Holden R (2011) Measuring the compactness of political districting plans. *The Journal of Law and Economics* 54(3): 493–535. DOI:10.1086/661511.

Gao S (2015) Spatio-Temporal analytics for exploring human mobility patterns and urban dynamics in the mobile age. *Spat. Cogn. Comput.* 15(2): 86–114. DOI:10.1080/13875868.2014.984300.

Gariazzo C, Pelliccioni A and Bogliolo MP (2019) Spatiotemporal analysis of urban mobility using aggregate mobile phone derived presence and demographic data: A case study in the city of rome, italy. *Brown Univ. Dig. Addict. Theory Appl.* 4(1): 8. DOI:10.3390/data4010008.

Ghahramani M, Zhou M and Hon CT (2018) Mobile phone data analysis: A spatial exploration toward hotspot detection. *IEEE Transactions on Automation Science and Engineering* 16(1): 351–362.

Giuliano G and Small KA (1991) Subcenters in the los angeles region. *Reg. Sci. Urban Econ.* 21(2): 163–182. DOI:10.1016/0166-0462(91)90032-I.

Guo C, Buchmann CM and Schwarz N (2019) Linking urban sprawl and income segregation – findings from a stylized agent-based model. *Environment and Planning B: Urban Analytics and City Science* 46(3): 469–489. DOI:10.1177/2399808317719072.

Hoteit S, Secci S, Sobolevsky S, Ratti C and Pujolle G (2014) Estimating human trajectories and hotspots through mobile phone data. *Computer Networks* 64: 296–307. DOI:10.1016/j.comnet.2014.02.011.

Huang J, Lu XX and Sellers JM (2007) A global comparative analysis of urban form: Applying spatial metrics and remote sensing. *Landsc. Urban Plan.* 82(4): 184–197. DOI:10.1016/j.landurbplan.2007.02.010.

INEGI (2010) Colección: Cartografía geoestadística urbana, cierre del censo de población y vivienda 2010. `https://www.inegi.org.mx/app/mapas/?t=0710000000000000&tg=3604`. Accessed: 2020-1-17.

Isaacman S, Becker R, Cáceres R, Martonosi M, Rowland J, Varshavsky A and Willinger W (2012) Human mobility modeling at metropolitan scales. In: *Proceedings of the 10th International Conference on Mobile Systems, Applications, and Services*, MobiSys '12. New York, NY, USA: ACM. ISBN 9781450313018, pp. 239–252. DOI:10.1145/2307636.2307659.

Kang C, Liu Y, Ma X and Wu L (2012) Towards estimating urban population distributions from mobile call data. *Journal of Urban Technology* 19(4): 3–21. DOI:10.1080/10630732.2012.715479.

Kubíček P, Konečný M, Stachoň Z, Shen J, Herman L, Řezník T, Staněk K, Štampach R and Leitgeb Š (2019) Population distribution modelling at fine spatio-temporal scale based on mobile phone data. *International Journal of Digital Earth* 12(11): 1319–1340. DOI:10.1080/17538947.2018.1548654.

Le Néchet F (2012) Urban spatial structure, daily mobility and energy consumption: a study of 34 european cities. *Cybergeo* DOI:10.4000/cybergeo.24966.

Li W, Chen T, Wentz EA and Fan C (2014) NMMI: A mass compactness measure for spatial pattern analysis of areal features. *Ann. Assoc. Am. Geogr.* 104(6): 1116–1133. DOI:10.1080/00045608.2014.941732.

Li W, Goodchild MF and Church R (2013) An efficient measure of compactness for two-dimensional shapes and its application in regionalization problems. *Int. J. Geogr. Inf. Sci.* 27(6): 1227–1250. DOI:10.1080/13658816.2012.752093.

Louail T, Lenormand M, Cantu Ros OG, Picornell M, Herranz R, Frias-Martinez E, Ramasco JJ and Barthelemy M (2014) From mobile phone data to the spatial structure of cities. *Sci. Rep.* 4: 5276. DOI:10.1038/srep05276.

Noulas A, Mascolo C and Frias-Martinez E (2013) Exploiting foursquare and cellular data to infer user activity in urban environments. In: *2013 IEEE 14th International Conference on Mobile Data Management*, volume 1. ieeexplore.ieee.org, pp. 167–176. DOI:10.1109/MDM.2013.27.

Openshaw S (1984) *The modifiable areal unit problem*. Norwich: Geo Abstracts Univ. of East Anglia.

Ouředníček M, Nemeškal J, Špačková P, Hampl M and Novák J (2018) A synthetic approach to the delimitation of the prague metropolitan area. *J. Maps* 14(1): 26–33. DOI:10.1080/17445647.2017.1422446.

Peredo OF, García JA, Stuven R and Ortiz JM (2017) Urban dynamic estimation using mobile phone logs and locally varying anisotropy. In: Gómez-Hernández JJ, Rodrigo-Ilarri J, Rodrigo-Clavero ME, Cassiraga E and Vargas-Guzmán JA (eds.) *Geostatistics Valencia 2016*. Cham: Springer International Publishing. ISBN 9783319468198, pp. 949–964. DOI:10.1007/978-3-319-46819-8_66.

Ratti C, Frenchman D, Pulselli RM and Williams S (2006) Mobile landscapes: Using location data from cell phones for urban analysis. *Environ. Plann. B Plann. Des.* 33(5): 727–748. DOI:10.1068/b32047.

Reades J, Calabrese F and Ratti C (2009) Eigenplaces: Analysing cities using the Space–Time structure of the mobile phone network. *Environ. Plann. B Plann. Des.* 36(5): 824–836. DOI:10.1068/b34133t.

Reades J, Calabrese F, Sevtsuk A and Ratti C (2007) Cellular census: Explorations in urban data collection. *IEEE Pervasive Comput.* 6(3): 30–38. DOI:10.1109/MPRV.2007.53.

Rubio A, Sanchez A and Frias-Martinez E (2013) Adaptive non-parametric identification of dense areas using cell phone records for urban analysis. *Eng. Appl. Artif. Intell.* 26(1): 551–563. DOI:10.1016/j.engappai.2012.05.005.

Sagl G, Delmelle E and Delmelle E (2014) Mapping collective human activity in an urban environment based on mobile phone data. *Cartogr. Geogr. Inf. Sci.* 41(3): 272–285. DOI:10.1080/15230406.2014.888958.

Scholz J, Andorfer M and Mittlboeck M (2013) Spatial accuracy evaluation of population density grid disaggregations with corine landcover. In: Vandenbroucke D, Bucher B and Crompvoets J (eds.) *Geographic Information Science at the Heart of Europe*. Cham: Springer International Publishing. ISBN 9783319006154, pp. 267–283. DOI:10.1007/978-3-319-00615-4_15.

Schwanen T, Dieleman FM and Dijst M (2001) Travel behaviour in dutch monocentric and policentric urban systems. *J. Transp. Geogr.* 9(3): 173–186. DOI:10.1016/S0966-6923(01)00009-6.

Schwarz N (2010) Urban form revisited—selecting indicators for characterising european cities. *Landsc. Urban Plan.* 96(1): 29–47. DOI:10.1016/j.landurbplan.2010.01.007.

Sevtsuk A and Ratti C (2010) Does urban mobility have a daily routine? learning from the aggregate data of mobile networks. *Journal of Urban Technology* 17(1): 41–60. DOI:10.1080/10630731003597322.

Statstutor (2020) Spearman's correlation. `http://www.statstutor.ac.uk/resources/uploaded/spearmans.pdf`. Accessed: 2020-1-17.

Strominger J, Anthopolos R and Miranda ML (2016) Implications of construction method and spatial scale on measures of the built environment. *Int. J. Health Geogr.* 15: 15. DOI:10.1186/s12942-016-0044-x.

Traag VA, Browet A, Calabrese F and Morlot F (2011) Social event detection in massive mobile phone data using probabilistic location inference. In: *2011 IEEE Third International Conference on Privacy, Security, Risk and Trust and 2011 IEEE Third International Conference on Social Computing*. pp. 625–628. DOI: 10.1109/PASSAT/SocialCom.2011.133.

Tranos E and Nijkamp P (2015) Mobile phone usage in complex urban systems: a space–time, aggregated human activity study. *J. Geogr. Syst.* 17(2): 157–185. DOI:10.1007/s10109-015-0211-9.

Trasarti R, Olteanu-Raimond AM, Nanni M, Couronné T, Furletti B, Giannotti F, Smoreda Z and Ziemlicki C (2015) Discovering urban and country dynamics from mobile phone data with spatial correlation patterns. *Telecomm. Policy* 39(3): 347–362. DOI:10.1016/j.telpol.2013.12.002.

Traunmueller M, Quattrone G and Capra L (2014) Mining mobile phone data to investigate urban crime theories at scale. In: *International Conference on Social Informatics*. Springer, pp. 396–411.

Tsai YH (2005) Quantifying urban form: Compactness versus 'sprawl'. *Urban Stud.* 42(1): 141–161. DOI: 10.1080/0042098042000309748.

Tu W, Cao J, Yue Y, Shaw SL, Zhou M, Wang Z, Chang X, Xu Y and Li Q (2017) Coupling mobile phone and social media data: a new approach to understanding urban functions and diurnal patterns. *Int. J. Geogr. Inf. Sci.* 31(12): 2331–2358. DOI:10.1080/13658816.2017.1356464.

Vieira MR, Frias-Martinez V, Oliver N and Frias-Martinez E (2010) Characterizing dense urban areas from mobile Phone-Call data: Discovery and social dynamics. In: *2010 IEEE Second International Conference on Social Computing*. pp. 241–248. DOI:10.1109/SocialCom.2010.41.

Wassmer RW (2000) Urban sprawl in a us metropolitan area: ways to measure and a comparison of the sacramento area to similar metropolitan areas in california and the us. *CSUS Public Policy and Administration Working Paper* (2000-03).

Xu W, Chen H, Frias-Martinez E, Cebrian M and Li X (2019) The inverted u-shaped effect of urban hotspots spatial compactness on urban economic growth. *R Soc Open Sci* 6(11): 181640. DOI:10.1098/rsos.181640.

Yang X, Fang Z, Xu Y, Shaw SL, Zhao Z, Yin L, Zhang T and Lin Y (2016) Understanding spatiotemporal patterns of human convergence and divergence using mobile phone location data. *ISPRS International Journal of Geo-Information* 5(10): 177. DOI:10.3390/ijgi5100177.

Zhao Z, Shaw SL, Xu Y, Lu F, Chen J and Yin L (2016) Understanding the bias of call detail records in human mobility research. *Int. J. Geogr. Inf. Sci.* 30(9): 1738–1762. DOI:10.1080/13658816.2015.1137298.

Zuo X and Zhang Y (2012) Detection and analysis of urban area hotspots based on cell phone traffic. *JCP* 7(7): 1753–1760.